

Firefly Assisted Genetic Algorithm for Selective Harmonic Elimination in PV Interfacing Reduced Switch Multilevel Inverter

Priyanka Sen*, Prabhat Ranjan Bana**[‡], Kaibalya Prasad Panda**

*Assistant Professor, Department of Electrical Engineering, C.V. Raman College of Engineering, Bhubaneswar, India, 752054

**Research Scholar, Department of Electrical Engineering, National Institute of Technology Meghalaya, Shillong, India, 793003

(psen466@gmail.com, prabhat.bana@nitm.ac.in, kaibalyapanda@nitm.ac.in)

[‡]Corresponding Author; Prabhat Ranjan Bana, Department of Electrical Engineering, National Institute of Technology Meghalaya, Shillong, India, Tel: +91 8658166477, prabhat.bana@nitm.ac.in

Received: 04.11.2018 Accepted: 30.12.2018

Abstract- The rapid advancement in the power electronic sector has evolved multilevel inverter (MLI) for different applications. Now a day's MLIs are chosen over the conventional two level inverters because of several advantages like less voltage stress, less electromagnetic interference, reduced filter size requirement, etc. However, the conventional MLIs require more device components to synthesize more levels. Considering this fact, this paper presents a novel 5-level MLI using fewer switch count suitable for standalone PV system. Furthermore, to effectively control and reduced the harmonics from the designed system, firefly assisted genetic algorithm (FAGA) based selective harmonic elimination (SHE) technique is developed. The targeted low-order harmonics from the output voltage of the proposed PV-MLI is eliminated using the FAGA algorithm. Existing firefly algorithm (FA) and genetic algorithm (GA) are also implemented for this purpose to verify the superiority of FAGA. Incremental conductance (IC) algorithm is used to yield the maximum power from the PV system. Simulation study of the overall system is carried out in MATLAB environment and the obtained results are discussed individually. An experimental test setup is developed finally to validate the working of PV integrated MLI with the SHE PWM control scheme which is further compared with the traditional PWM control technique.

Keywords—Firefly assisted genetic algorithm (FAGA); maximum power point tracking (MPPT); multilevel inverter (MLI); photovoltaic (PV) system; selective harmonic elimination (SHE).

1. Introduction

Tremendous growth in renewable energy source based electrical energy production in the recent past has motivated research interest among power electronics and power system communities. Due to the low efficiency of generation, high cost of fuel, and high losses, fossil fuels are ineptitude to meet the power demand [1]–[3]. Extensive use of fossil fuel will also result in global warming and also in the near future, it is expected that fossil fuel may completely be drained out from the earth. In this perspective, renewable energy sources like solar photovoltaic (PV) and wind energy have emboldened as an alternative to the fossil fuel based system of electricity generation. To extract utmost power, especially from the PV sources, rapid advancement in the power converters, semiconductor technologies, and control techniques can be noticed [4], [5]. The output voltage of the PV array is very less in magnitude and is fluctuating in

nature which can be improved by employing a dc-dc converter. Different maximum power point tracking (MPPT) [6], [7] algorithms can also be implemented in the converter in order to extract the maximum efficiency from the PV array.

The dc power produced by the PV array has to be converted to ac before feeding it to the grid or ac load. Conventional three-level inverters are widely used in the inversion stage, but their efficiency is limited and also have high voltage stress, and electromagnetic interference [8], [9]. In this aspect multilevel inverters (MLI) are gaining more attention in the small to large scale industry as well as commercial applications. The attractive feature of the MLI is that it has the ability to operate at both high switching and fundamental switching frequency with an exceptional harmonic profile [10]. Neutral point clamped or diode-clamped multilevel inverters (DC MLI), capacitor clamped multilevel inverters (CC MLI) and cascaded H-bridge type

multilevel inverters (CHB MLI) are the major types of MLI used for dc-ac conversion process [11]–[13]. Less utilization of switching devices and dc voltage sources can assist a particular MLI structure to produce a number of levels at the output with less voltage stress. DC MLI and CC MLI structures involve more diodes count and a number of capacitors to synthesize higher levels at output thus voltage balancing, structural complexity, bulky, and more cost are the major drawbacks of these topologies [11], [14]. Hence, these MLI types are not the recommended for use in higher level applications. On contrary CHB MLI utilizes fewer components (no need of clamping capacitors and clamping diodes) among all the conventional MLI structures and it can be easily modularized [12], [15], [16].

These MLIs require isolated dc sources to synthesize multiple voltage levels at the output, which makes it more popular in the solar PV application. The major disadvantage of all the conventional MLI topologies is that, they require greater number of switching devices to synthesize more levels at the output. Hence the current research is focused on reduction of requirement of sources and switching components, so that the size and cost of a MLIs can be reduced [17], [18]. In this regard, one reduced switch MLI is proposed in this paper which counters the aforementioned drawbacks.

Several well developed control techniques for controlling the MLI with an aim to reduce the total harmonic distortion (THD) [19]–[21] has been presented in the literature. They all fall under two categories such as: low or fundamental and high switching frequency control techniques. High switching frequency control techniques are popular in minimizing the especially the current THD to a low value. However, more switching loss is the major concern in such techniques which makes the low/fundamental switching frequency control techniques superior in this aspect. Selective harmonic elimination (SHE) is a very famous fundamental switching control scheme which has the ability to completely eliminate the targeted dominant lower order harmonics thereby reducing the THD to a very low value. SHE technique involves a set of trigonometric Fourier series transcendental equations which needs to be solved in order to obtain the accurate switching angles. The nonlinear equations can be solved by conventional methods such as Newton-Raphson, polynomial method [19], [22]. But the solution obtained using these methods depend upon the appropriate initial guess hence accuracy of these methods is very less and also implementation in real-time is more difficult. This problem can be avoided by treating it as an optimization problem instead of algebraic numericals.

Different optimization algorithms implemented in the literature to obtain the optimum switching angles are; colonial competitive algorithm (CCA) [23], particle swarm optimization (PSO) [24], [25], genetic algorithm (GA) [10], [26], [27], firefly algorithm (FA) [28], etc. FA is based on the nature of fireflies. It can give the desired firing angle in less computation time which is because of its natural subdivision and capability of working with several modes.

FA operate on the principle of reduction of attractiveness with the reduction in distance. Hence the whole population can be naturally separated into smaller groups and each group will search around local optima, and in a result the best solution can be obtained. The main problem of this algorithm is the absence of memory and slow convergence rate due to which, while solving a multi-optimum problem, it stuck around some local minima [28]. FA cannot remember the previously obtained better solution by each firefly. So they may end their search with missing their desired solution. To overcome these problems GA concept can be hybridized with FA. GA has high convergence rate, unlike the FA and it does not confine to the local minima. The crossover and mutation operator of GA can search new solution. In this paper, Firefly assisted Genetic algorithm (FAGA) is implemented to solve the nonlinear equations involved in SHE technique. The best solutions chosen by FA will be the initial population for GA.

The paper is organized as follows: Section 2 includes detailed analysis of the components involved in the proposed system configuration. In section 3, operating principle of the proposed MLI is discussed. This section also includes comparison among the proposed MLI and different well-known MLI topologies. Section 4 introduces the proposed FAGA approach for solving SHE problem. A comparative analysis of FAGA, FA, and GA algorithms is addressed in section 5. The obtained simulation results are discussed in section 6 and prototype of the proposed MLI is developed to validate the simulation findings in Section 7. At last the conclusion is drawn on the aforementioned subjects in section 8.

2. Proposed System Analysis

Power quality improvement of the solar PV system is a major concern in the present scenario. In this regard, the proposed system configuration to enhance the quality of the power produced from the solar PV system is depicted in Fig. 1.

2.1. PV Cell Modelling

The equivalent circuit of PV system shown in Fig. 1 can be a single diode model or a two diode model. The two diode model requires more parameters in order to appropriately design the equivalent model [29]. Hence single diode model is generally preferred. The output current expression of such a model can be given as:

$$I = I_{pv} - I_D - \left(\frac{V + I_{pv}R_s}{R_{sh}} \right) \quad (1)$$

where I_D is the current through the diode which can be expressed in Eq. (2).

$$I_D = I_o \left[\exp \left(\frac{V + I_{pv}R_s}{aV_T} \right) \right] \quad (2)$$

where, I_{pv} = current produced by the PV module, I_o = reverse saturation current of diode, $V_T = NKT/q$ = thermal voltage of the PV module, N = number of cells connected in series, q = charge of electron, K = Boltzmann constant, a = ideality constant of the diode

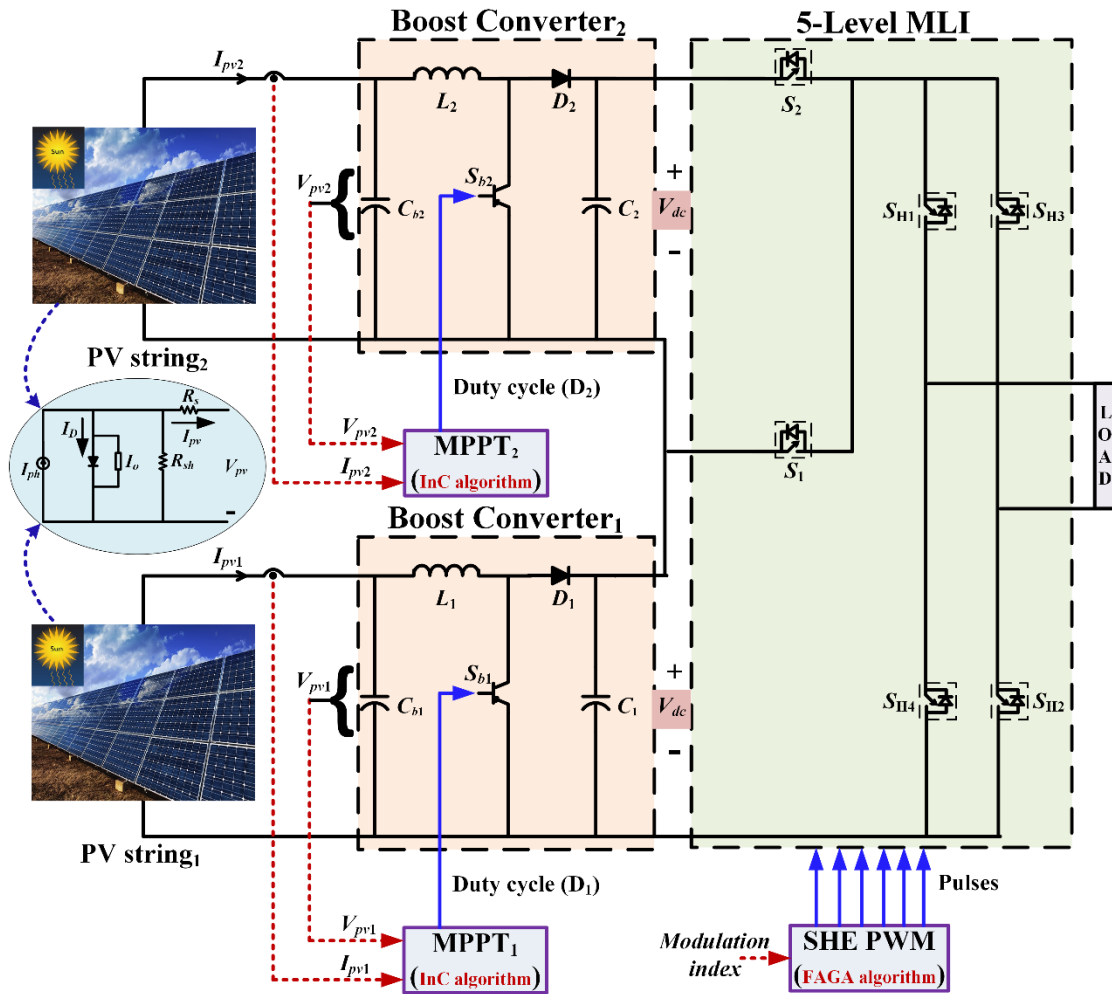


Fig. 1. Overall two-stage PV integrated MLI system design

2.2. Maximum power point tracking (MPPT)

The efficiency of the solar PV panel is very less, hence MPPT control technique is normally employed to operate the PV sources at maximum power point (MPP). MPP indicates the operating point where maximum power or efficiency can be achieved from the PV sources. With the advancement in power electronic sector, MLI with MPPT technique in the dc-dc converter is a better combination to extract the utmost power with improved quality of a PV integrated system. For this purpose several MPPT algorithms like incremental conduction (IC), perturb & observe (P&O) method, etc., are frequently used for uniform shading condition. However, they fail to operate at global MPP during partial shading condition. Fuzzy logic [30], [31] and neural network [32] based MPP tracking techniques have been thus analyzed to efficiently track the global peak operating point of the PV system. However, the former approach involves large computational analysis for fuzzification and defuzzification process. Furthermore the neural network based approach to track the global peak among multiple peaks during partial shading require huge data based training process. Due to requirement of large data processing, these control techniques also suffers from extreme computational burden and large data storage on the processor issues. To avoid such problem, several optimization algorithms based MPPT technique has been reported in the literature [6], [7]. Researchers are also involved in reduction of complexity,

sensing element requirement, etc., in order to make the system simple and cost effective [33].

In this work IC method [34] is focused considering uniform shading condition. Following are the conventional set of equations concluded from the power-voltage curve of the PV source.

$$\frac{dP}{dV} = 0 \text{ at MPP, } \frac{dP}{dV} > 0 \text{ left to MPP, and } \frac{dP}{dV} < 0 \text{ right to MPP} \quad (3)$$

The relationship between power, voltage, and current can be expressed as:

$$\frac{dP}{dV} = \frac{d(VI)}{dV} = I + V \frac{dI}{dV} \cong I + V \frac{\Delta I}{\Delta V} \quad (4)$$

where $\Delta I/\Delta V$ is the incremental conductance rate.

From Eq. (3), MPP is the point where dP/dV become zero. Considering this, the set of equations involved in IC method to locate the MPP can be expressed as:

$$\frac{dI}{dV} = -\frac{I}{V} \text{ at MPP, } \frac{dI}{dV} > -\frac{I}{V} \text{ left of MPP, } \frac{dI}{dV} < -\frac{I}{V} \text{ right of MPP} \quad (5)$$

Thus, by comparing conductance (I/V) and incremental conductance ($\Delta I/\Delta V$) and equalizing the summation of both

of them to zero, the maximum power point can be tracked easily. Hence, the error obtained with this method in tracking the MPP can be given as per Eq. (6) which can be considerably minimized by using any type of controller.

$$e = -\frac{i}{v} + \frac{\Delta i}{\Delta v} \tag{6}$$

2.3. DC-DC Converter

In order to minimize the ripple produced in the output voltage of the PV array, dc-dc converters are used. Normally the dc-dc converter is classified as: buck converter or step down converter, boost converter or step up converter and buck-boost converter or isolated converter. Each one has their advantage in their own way. In this paper boost converter is utilized as dc-dc interface before the inversion stage. It is operated in continuous conduction mode, which helps in boosting the lower magnitude PV output voltage. The regulated dc output voltage of the boost converter is then given to the proposed MLI.

3. Proposed 5-level MLI (P5M) Structure

The traditional CHB MLI requires $(m-1)/2$ number of dc sources and $2(m-1)$ number of switches to synthesize an m -level output. Moreover to generate a 5-level output, CHB MLI utilizes 8 numbers of switches. These switches further require same number of gate drive circuits thus making the MLI topology more costly. In this aspect one reduced switch MLI is proposed in this work which requires only 6 switches to synthesize a same 5-level output.

The proposed 5-level MLI (P5M) structure is shown in Fig. 1. S_1 and S_2 are the level generating switches which are combined with the polarity generation switches S_{H1} , S_{H2} , S_{H3} , and S_{H4} . The switching combination for getting different levels is detailed in Table 1. S_{H1} and S_{H2} remain in ON state for the positive polarity generation. In such a case, when the switch S_1 is turned ON, then $+V_{dc}$ will be obtained at output. Making the switch S_2 ON, the voltage level of $+2V_{dc}$ will be obtained at the output. Similarly the negative voltage levels can be obtained by keeping the switches S_{H3} , and S_{H4} in ON state. In this process the switches from the same leg should not be turned ON simultaneously or else it will lead to a short circuit of the source side circuit. The zero level can be obtained by keeping the switches S_{H1} and S_{H3} in conducting state. The generalized expression of the requirement of different components by the P5M structure is given in the following equations.

$$N_{dc} = \frac{m-1}{2} \tag{7}$$

$$N_{sw} = \frac{m+7}{2} \tag{8}$$

$$N_{driver} = N_{sw} \tag{9}$$

where N_{dc} , N_{sw} , and N_{driver} are the number of dc sources, switch count, and driver circuit count, respectively. In order to prove the effectiveness of the P5M topology, it is compared with some recently developed MLI topologies which are given in Table 2.

Table 1. Switching pattern for P5M topology

V _{OUT}	1 represents the switch ON condition & 0 represents the switch OFF condition					
	Main switches		Common switches			
	S_1	S_2	S_{H1}	S_{H2}	S_{H3}	S_{H4}
V_{dc}	1	0	1	1	0	0
$2V_{dc}$	0	1	1	1	0	0
0	0	0	1	0	1	0
$-V_{dc}$	1	0	0	0	1	1
$-2V_{dc}$	0	1	0	0	1	1

Table 2. Comparison between 5-level MLI structures

Parameter	CHB MLI [11], [12], [35]	MLI 1 [10]	MLI 2 [36]	MLI 3 [37]	MLI 4 [38]	MLI 5 [39]	P5M topology
N_{dc}	2	2	2	2	2	2	2
N_{sw}	8	8	8	8	7	7	6
N_{driver}	8	8	8	8	7	7	6
m	5	5	5	5	5	5	5

4. Firefly Assisted Genetic Algorithm (FAGA)

4.1. Description of proposed FAGA approach

FA is a meta-heuristic algorithm based on the flashing characteristics of fireflies [40] first implemented by Xin-She Yang. The fireflies exhibit a unique behavior of producing a particular pattern of flash which, if implemented mathematically then it can yield the optimum solutions for the nonlinear equations. The nature of the fireflies has three directions. The first direction is that all the same sex fireflies move towards each other and as they all are about same sex hence their movement doesn't get affected by the sex which in turn eliminates the problem of occurrence of crossover unlike GA. The second direction is the movement of firefly towards the nearer and brighter firefly which occurs as a function of the distance between each firefly and the brightness of each fly. Sometimes they find difficulties for identification of brighter fly, which makes them move randomly. Their random movement is an ordered one based on the intensity of their light which cannot be sensed by human eyes. The third direction is that the value of objective function involved to each fly is associated with the intensity of the light emission of the individual firefly.

If Y_r and Y_s are the positions of two firefly 'r' and 's' respectively, then the degree of attractiveness between them can be expressed as;

$$A = A_o e^{-l(z_{rs})^k}, \quad k \geq 1 \quad (10)$$

$$Z_{rs} = |Y_r - Y_s| \quad (11)$$

where, Z_{rs} = Distance between the two flies, l = Absorption coefficient, A = Degree of attractiveness, A_o = Initial attractiveness, ' l ' control the reduction of light intensity whose value always lies between 0 and 10. The value of A_o is chosen nearly to 1, so that the position of other flies in its neighborhood can be determined by the brightest firefly. By taking the assumption that the brightness of firefly 'r' is less than that of 's', the new position of firefly 'r' is expressed as follows;

$$Y_r^{t+1} = Y_r^t + A(Y_r - Y_s) + c(R - \frac{1}{2}) \quad (12)$$

where c is the random movement factor and R is a random number. The value of R is chosen as higher value for the global search space and a smaller value can be considered for the local search space. Moreover, its value lies in between 0 and 1. The value of c is again a random number which can be determined from the problem of interest.

Although the FA is beneficial due to its simple and robust nature, but there are certain problems involved in FA such as leisurely convergence, lack of memory capability and sometimes it is trapped in local minima point. On the other hand GA has the ability to move out from the local minima point. GA [10], [41], [42] is basically based upon the natural selection, a process wherein a competitive environment the strongest participants are the winners. To overcome the aforementioned problems associated with FA, GA can be smartly combined with FA.

The proposed FAGA works in two basic steps. In the first step, FA work and produce the best solutions. In the second step the solutions obtained from the FA are utilized as initial population for GA. At the end of running of GA, the solutions obtained are treated as the desired optimum solution at the minimum value of the objective function. The flowchart overview of the FAGA algorithm is illustrated in Fig. 2.

4.2. Application of FAGA for SHE

The output voltage waveform of an inverter exhibit odd symmetric property, thus the generalized Fourier series expression of the MLI output voltage can be mathematically expressed as in Eq. (13) and the peak voltage of x^{th} harmonics in Eq. (14).

$$V(\omega t) = \sum_{x=1,3,5}^{\infty} V_x \sin(x\omega t) \quad (13)$$

$$V_x = \begin{cases} \frac{4V_{dc}}{x} [\cos x\alpha_1 + \cos x\alpha_2] & \text{for odd } x \\ 0 & \text{for even } x \end{cases} \quad (14)$$

subject to the constraint,

$$0 < \alpha_1 < \alpha_2 \leq 90 \quad (15)$$

where, V_x = magnitude of x^{th} harmonic, ω = fundamental switching frequency, α = switching angle

Following set of equations can be formulated to eliminate the 5th order harmonic as well as to keep the fundamental component unaffected.

$$V_1 = \cos \alpha_1 + \cos \alpha_2 = 3M \quad (16)$$

$$V_5 = \cos \alpha_1 + \cos \alpha_2 = 0 \quad (17)$$

where, M = Modulation index and can be determined as $M = V_d/4N_{dc}(V_{dc}/\pi)$, $0 < M < 1$, V_d = desired fundamental component

The main objective of the FAGA is to obtain the optimum switching angles (α_1 and α_2) by solving the nonlinear equations stated in Eq. (16) & (17) for which the targeted 5th order harmonic can be effectively eliminated. An objective function (OF) needs to be defined to obtain optimum solution as well as to maintain the desired fundamental component. The considered OF is given in Eq. (18). To limit the error in fundamental and the 5th order harmonics to very low value, i.e., about 1%, H is taken as 0.01.

$$OF = \frac{1}{H} * \left[\left| M - \frac{|V_1|}{N_{dc}V_{dc}} \right| + \left(\frac{|V_5|}{N_{dc}V_{dc}} \right) \right] \quad (18)$$

5. Comparison of FAGA with FA and GA

The proposed FAGA algorithm is coded in MATLAB R2017a environment to determine the optimized switching angle for proposed MLI. In order to prove the superiority of the proposed FAGA approach, both FA and GA are also implemented in the same environment. The parameters that are considered for the FAGA algorithm are: FA ($l = 1$, $A_o = 0.98$, $k = 2$, $c = 0.2$, fireflies count = 100, iteration count = 200), GA (probability of crossover and mutation = 0.2 & 0.02, population size = 100, generation count = 200).

Minimizing the objective function to a lower value always proves the effectiveness of an optimization algorithm. In this perspective the logarithmic value of the objective function versus the change in modulation index is obtained using all three algorithms and is illustrated in Fig. 3(a). From this plot, it can be said that GA and FA are able to minimize the objective function to below 10^{-4} and 10^{-21} respectively. At the same time the proposed FAGA algorithm is minimizing the objective function below 10^{-37} over the 95% variation range of modulation index. Hence, it can be concluded that

FAGA algorithm has the greater tendency to obtain an optimal solution as compared with the other two algorithms.

Fig. 3(b) shows the optimum switching angles versus modulation index obtained using FAGA. Modulation index is varied over a range of 0 to 1. The obtained switching angle satisfies the equation stated in (15) for all the varied value of M . It can be observed that switching angles are inversely proportional to the M , i.e., with the increment in M , switching angle values gradually decreases and also shifts nearer to the origin.

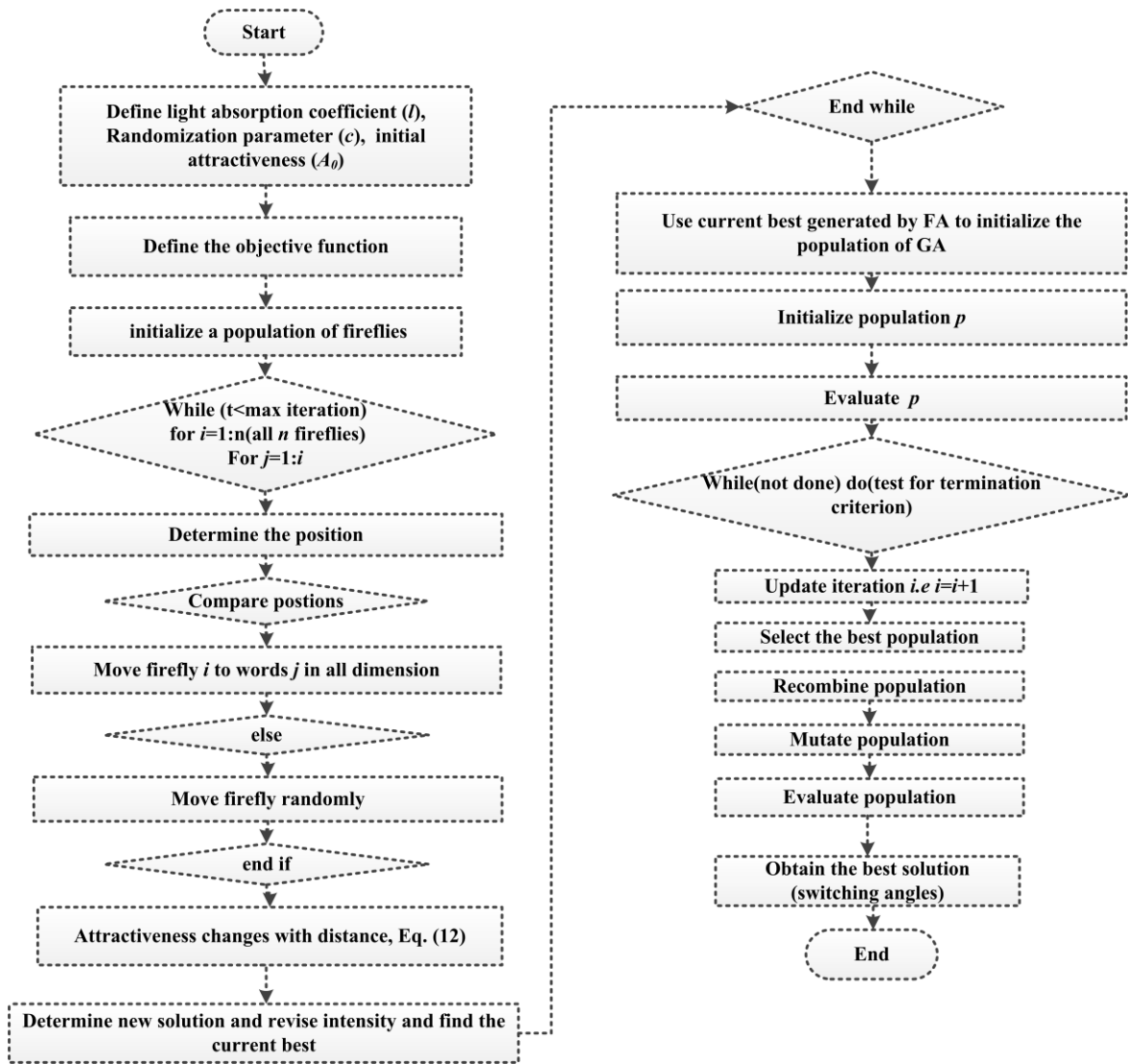


Fig. 2. Flowchart of proposed FAGA algorithm

THD indicates the measure of voltage quality of an inverter. Obtained THD with all the three algorithms versus modulation index is illustrated in Fig. 3(c) from which it can be clearly marked that the proposed FAGA performs superior than FA and GA in minimizing the THD to a very low value. In such a case M is varied in the range of 0 to 1 with a step size of 0.01. With the increase in modulation index, the percentage THD decreases. Thus operating the MLI at high modulation index, i.e., near to unity is always preferred. To have an effective understanding on the successfulness of FAGA in elimination of low order

harmonics, extracted harmonic amplitude versus modulation index is shown in Fig. 3(d). The amplitude of 3rd harmonic is decreasing with the increase in modulation index and amplitude of 5th harmonic is getting completely eradicated for the modulation index value greater than 0.7.

From the above comparative analysis, it is clearly evident that FAGA takes lesser time to converge an optimum solution than GA and FA. It also helps in obtaining the accurate, stable switching angles by solving the nonlinear equations.

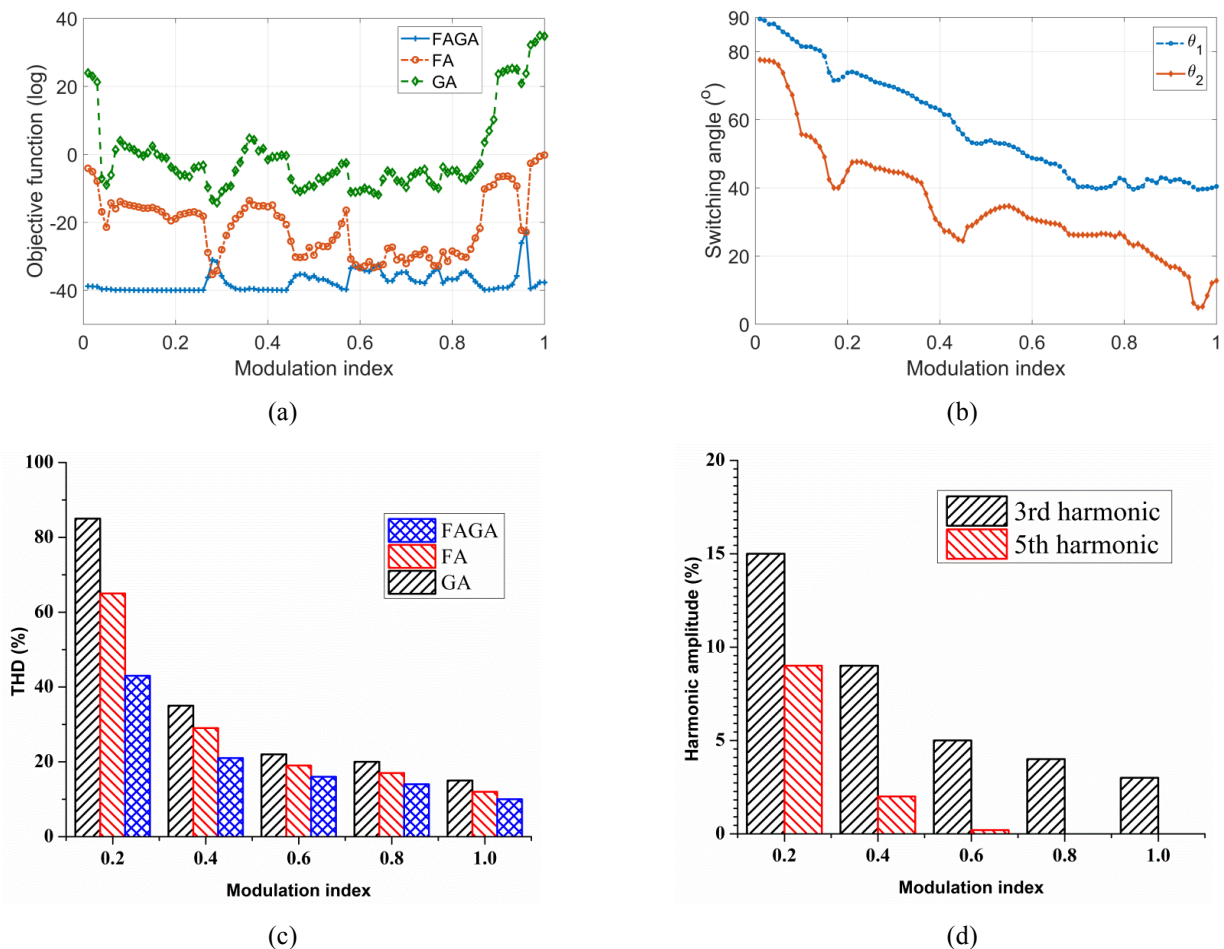


Fig. 3. Results obtained using programming (a) objective function against M, (b) switching angles against M using FAGA, (c) THD Vs M, (d) 3rd and 5th harmonics against M using FAGA

6. Simulation Results

The system configuration as shown in Fig. 1 is developed and simulated in MATLAB 2017 Simulink environment. The parameters considered in simulation and experimental validation are given in Table 3. To generate the appropriate switching pulses for the transistors used in the converters, IC algorithm is coded with a purpose to track the MPP under the adverse environmental condition. However, it can be noted that more efficient and well established algorithms can be implemented to obtain a better response in

Table 3. Parameters of the PV-MLI system designed

Solar Panel (2 X 1 in each string)			Boost Converter (Using MOSFET switch)			MLI (Using IGBT switches)		
Parameters	Simulation	Experimental	Parameters	Simulation	Experimental	Parameters	Simulation	Experimental
P_m (W)	60	8.3	L_1 (μ H)	220	150	V_{dc} (V)	70	25
V_{oc} (V)	21.1	8	L_2 (μ H)	220	150	f (Hz)	50	50
I_{sc} (A)	3.8	1.4	C_{bl} (μ F)	430	80	C_l (μ F)	2200	1500
V_{mp} (V)	17.1	6.4	C_{bl} (μ F)	430	80	Load (R) (Ω)	120	100
I_{mp} (A)	3.5	1.3	f_{sb} (kHz)	20	16	Load (L) (mH)	150	120

terms of tracking of global MPP. In such a case, the switching frequency of both the transistors is considered as 20 kHz. The output of both the boost converters acts as input to the proposed reduced switch 5-level inverter. The effectiveness of SHE technique is discussed in the earlier section which is adopted here to yield the switching pulses for the proposed MLI by targeting to eliminate the 5th order harmonics. The proposed FAGA algorithm is used to obtain the definite solution of the nonlinear transcendental equations involved in the SHE technique.

Considering the fact of dynamic behavior of atmospheric condition, all the results are obtained at the changing irradiance level under uniform shading of PV modules. The atmospheric temperature is kept fixed at 25 °C for this purpose. The irradiance and temperature profile is depicted in Fig. 4(a) indicates that there is a sudden decrement in irradiance level from 1000 W/m² to 700 W/m². The obtained voltage, current, and duty cycle of each individual PV modules (PV string-1 and PV string-2) are depicted in Fig. 4(b) and 4(c), respectively from which it can be inferred that, due to the change in irradiance level at 0.5 s, the current suddenly falls, however due to appropriate working of MPPT controller (i.e., by generation of new duty cycle) voltage profile of PV module is maintained stable.

The total power is nothing but the summation of all power produced by individual PV panels which can be verified from the Fig. 4(d). Fig. 5(a-d) shows the actual and zoomed version of the output voltage and the load current waveforms which reflects the change in irradiance level. The dc-link voltages are the input to the proposed MLI. As shown in Fig. 5(e) both the dc-link voltages are maintained stable at a same value and thus a total peak of about 145 V is obtained at the output. In order to verify the effectiveness of the proposed FAGA algorithm, FFT analysis of the output voltage waveform is carried out as shown in Fig. 5(f) in which the targeted dominant 5th order harmonic is completely eradicated thus the obtained THD without the use of large filters is very low value of 13.19 %.

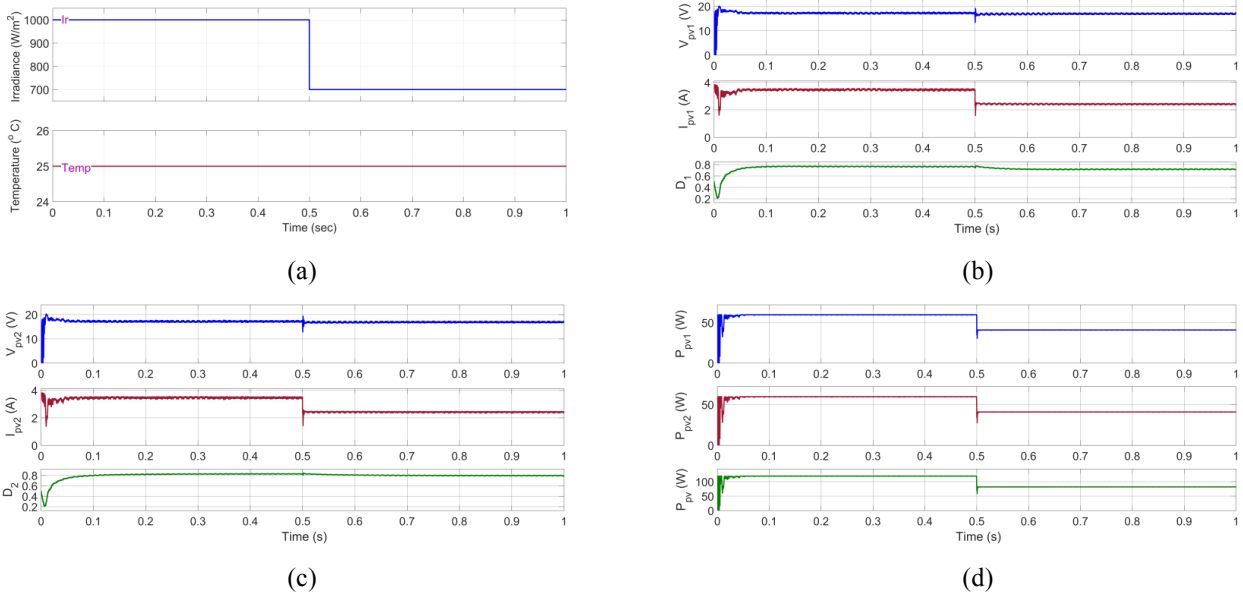
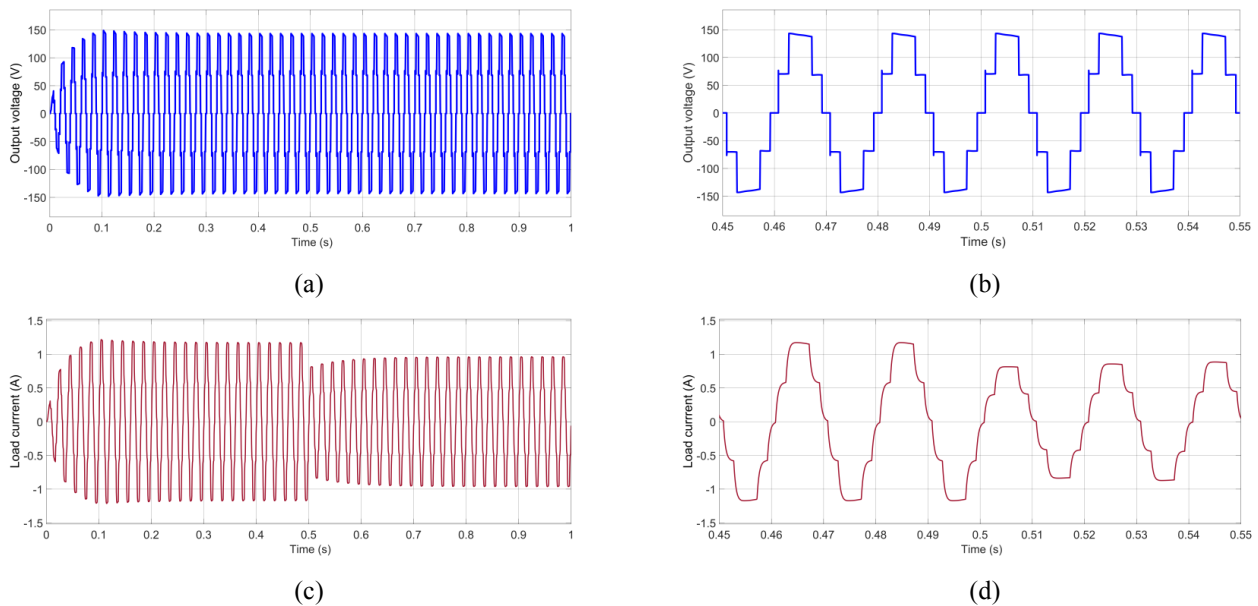
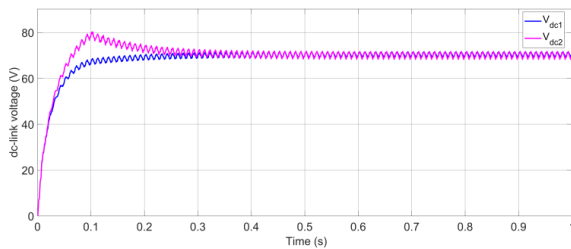
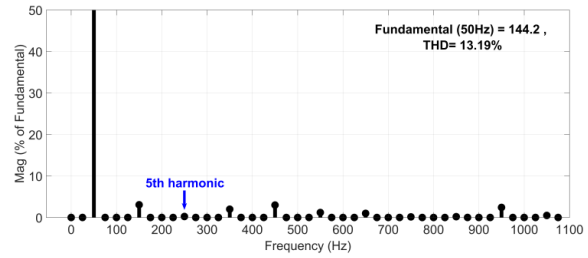


Fig. 4. Simulation results: (a) temperature and irradiance profile, (b) PV panel-1 parameters, (c) PV panel-2 parameters, (d) total PV output power





(e)



(f)

Fig. 5. Simulation results: (a) output voltage (V_o) (b) zoomed view of V_o , (c) output current (I_o), (d) zoomed view of I_o , (e) dc-link voltages, (f) THD analysis of V_o

7. Experimental Results and Discussion

A prototype model of the proposed system configuration is developed in the laboratory to validate the simulated and theoretical analysis. The overall test setup is shown in Fig. 6. PV panels are connected with two individual boost converters. The real-time switching pulses for the boost converters, including proposed MLI are generated by the controller Arduino ATmega 2560 where the control algorithms are accurately coded. All the parameter values that are considered for the above purpose are tabulated in Table 3. Two IRF540 metal oxide semiconductor field effect transistors (MOSFETs) are utilized for the design of the boost converters. The boost converter switching frequency is chosen as 16 kHz and operated in the continuous conduction mode. Furthermore PV voltage and current are fed into the controller to successively execute the MPPT algorithm. For this purpose scaled down reference voltage based voltage divider and ACS712 current sensors are used to sense the PV voltage and current, respectively. The proposed MLI is integrated with the above designed PV system. Six IRGP4050 insulated gate bipolar transistors (IGBTs) are used to construct the proposed MLI. A nominal frequency of 50 Hz is considered for the inverter output. As earlier mentioned, FAGA algorithm is executed in the controller to generate the desired pulses for the six switches which are driven by the TLP250 based driver circuit. All the experimental waveforms are acquired with oscilloscopes TDS 2024 and WT 1800 power quality analyzer.

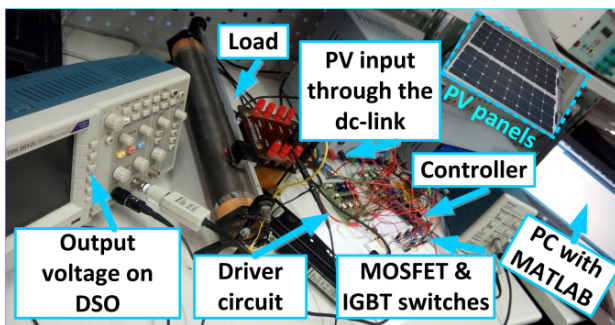


Fig. 6. PV-MLI experimental test setup in the laboratory

At first MPPT performance is evaluated experimentally with an assumption that, the PV panels are uniformly shaded and atmospheric temperature is 25 °C. Under this condition the output voltage and current of the PV system is shown in Fig. 7(a). It can be marked that, due to the sudden decrement

in irradiance level from 900 W/m² to 700 W/m² the current also decreases with a same proportion. However, the voltage is maintained constant by the boost converter employed with IC algorithm. From the calculated power curve it is clearly visible that, oscillations are less even after the change of irradiance level, which comes into a stable position after some time indicating the successful execution of IC algorithm. Negligible oscillations is present in the power curve around the MPP which can be completely eradicated employing more efficient MPPT algorithms. A similar test is again carried out countering the sudden increase and decrease in environmental effect and the resulted change in current, voltage, and the power curve is depicted in Fig. 7(b). In this case, the irradiance is suddenly changed to 800 W/m² from 200 W/m² and then to 200 W/m².

Furthermore, to verify the working principle of proposed MLI, tests have been carried out considering both fundamental switching PWM control technique as well as high-frequency switching PWM control technique. Traditional carrier-based sinusoidal PWM (SPWM) control technique is implemented taking 2 kHz switching frequency and modulation index nearly equals to 1. Fig. 7(c) and 7(d) shows the 5-level output voltage, current, and the corresponding voltage harmonic profile obtained using the proposed FAGA approach and SPWM technique, respectively. It is important to note that lesser voltage THD is obtained using FAGA SHE PWM (THD = 13.26%) control technique compared to the SPWM technique (THD = 15.01%). This is due to increase in the fundamental voltage level and elimination of targeted dominant harmonic orders from the output voltage. But, improved current waveform is obtained using SPWM technique due to high-frequency switching. However, the switching losses resulted using the traditional SPWM control technique will be very high compared to the proposed technique.

The 3rd order harmonic component can be inherently eliminated from the line-line voltage of a three phase system. Hence 5th order harmonic component is targeted here for elimination. The resulted harmonic profile proves the aggressiveness of the proposed FAGA algorithm in mitigating the targeted harmonic component in addition to maintaining the fundamental voltage level. Though FFT analysis of only the voltage waveform is carried out, but it can be said that, current THD value will be very less due to the filtering ability of a practical inductive type load.

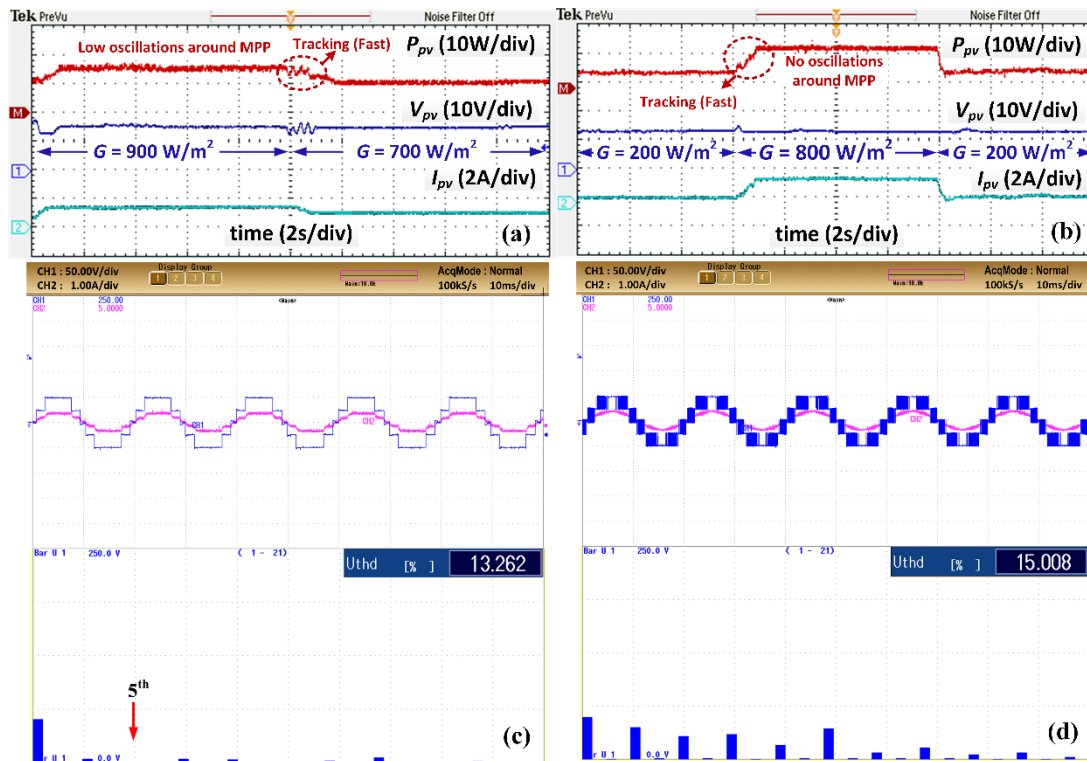


Fig. 7. Experimental results: (a) MPP tracking performance during step decrease of irradiance, (b) MPP tracking performance during sudden irradiance change, (c) V_o & I_o using SHE PWM and THD analysis of V_o , (d) V_o & I_o using SPWM and THD analysis of V_o

8. Conclusion

A novel 5-level MLI based standalone PV system was developed in this paper. The proposed MLI can easily be modularized to any number of levels as per the requirement. The key advantage of the proposed MLI is that, it utilizes a fewer number of switching devices to realize more levels in the output voltage waveform. Moreover, it avoids the major issues such as complexity in structure, high voltage stress on the switches, thus it is best suitable for medium-high voltage level applications. SHE PWM switching scheme based on FAGA algorithm for the proposed MLI structure to generate a 5-level output was analyzed. Furthermore FAGA algorithm accurately solves the nonlinear equation related to SHE technique resulting in complete elimination of targeted lower order harmonic. The superiority of the FAGA algorithm was validated with two conventional existing algorithms, i.e., FA and GA. Under uniformly shaded condition of the PV system, IC MPPT algorithm suitably generates switching pulse for the boost converter which also maintains the stable dc-link voltage. It is worth noting that, more established MPPT algorithms can be implemented to track the global MPP under partial shading condition. A detailed simulation study of each stage of the proposed system configuration was carried out for the validation. Experimental tests confirm the efficacy of designed system with the SHE PWM control scheme as well as traditional SPWM control scheme.

References

[1] K. W. Kow, Y. W. Wong, R. K. Rajkumar, and R. K. Rajkumar, "A review on performance of artificial intelligence and conventional method in mitigating PV

grid-tied related power quality events," *Renewable and Sustainable Energy Reviews*, vol. 56, pp. 334–346, Apr. 2016.

[2] O. P. Mahela and A. G. Shaik, "Comprehensive overview of grid interfaced solar photovoltaic systems," *Renewable and Sustainable Energy Reviews*, vol. 68, pp. 316–332, Feb. 2017.

[3] S. Hakimizad, S. R. Asl, and M. M. Ghiai, "A Review on the Design Approaches Using Renewable Energies in Urban Parks," *International Journal of Renewable Energy Research (IJRER)*, vol. 5, no. 3, pp. 686–693, Sep. 2015.

[4] C. Cecati, F. Ciancetta, and P. Siano, "A Multilevel Inverter for Photovoltaic Systems With Fuzzy Logic Control," *IEEE Transactions on Industrial Electronics*, vol. 57, no. 12, pp. 4115–4125, Dec. 2010.

[5] S. K. Chattopadhyay and C. Chakraborty, "A New Asymmetric Multilevel Inverter Topology Suitable for Solar PV Applications With Varying Irradiance," *IEEE Transactions on Sustainable Energy*, vol. 8, no. 4, pp. 1496–1506, Oct. 2017.

[6] J. P. Ram, T. S. Babu, and N. Rajasekar, "A comprehensive review on solar PV maximum power point tracking techniques," *Renewable and Sustainable Energy Reviews*, vol. 67, pp. 826–847, Jan. 2017.

[7] B. Subudhi and R. Pradhan, "A Comparative Study on Maximum Power Point Tracking Techniques for Photovoltaic Power Systems," *IEEE Transactions on Sustainable Energy*, vol. 4, no. 1, pp. 89–98, Jan. 2013.

- [8] V. F. Pires, D. M. Sousa, and J. F. Martins, "Three-phase nine switch inverter for a grid-connected photovoltaic system," in *2013 International Conference on Renewable Energy Research and Applications (ICRERA)*, 2013, pp. 1078–1083.
- [9] Y. Fayyad and L. Ben-Brahim, "Multilevel cascaded Z source inverter for PV power generation system," in *2012 International Conference on Renewable Energy Research and Applications (ICRERA)*, 2012, pp. 1–6.
- [10] S. S. Lee, B. Chu, N. R. N. Idris, H. H. Goh, and Y. E. Heng, "Switched-Battery Boost-Multilevel Inverter with GA Optimized SHEPWM for Standalone Application," *IEEE Transactions on Industrial Electronics*, vol. 63, no. 4, pp. 2133–2142, Apr. 2016.
- [11] J. Rodriguez, J.-S. Lai, and F. Z. Peng, "Multilevel inverters: a survey of topologies, controls, and applications," *IEEE Transactions on Industrial Electronics*, vol. 49, no. 4, pp. 724–738, Aug. 2002.
- [12] K. P. Panda and S. K. Mohapatra, "Anti-predatory PSO technique-based solutions for selected harmonic elimination in cascaded multilevel inverters," *International Journal of Industrial Electronics and Drives*, vol. 3, no. 2, pp. 78–88, Jan. 2016.
- [13] E. Kabalci, Y. Kabalci, R. Canbaz, and G. Gokkus, "Single phase multilevel string inverter for solar applications," in *2015 International Conference on Renewable Energy Research and Applications (ICRERA)*, 2015, pp. 109–114.
- [14] H. R. Massrur, T. Niknam, M. Mardaneh, and A. H. Rajaei, "Harmonic Elimination in Multilevel Inverters Under Unbalanced Voltages and Switching Deviation Using a New Stochastic Strategy," *IEEE Transactions on Industrial Informatics*, vol. 12, no. 2, pp. 716–725, Apr. 2016.
- [15] Y. Sinha and A. Nampally, "Modular multilevel converter modulation using fundamental switching selective harmonic elimination method," in *2016 IEEE International Conference on Renewable Energy Research and Applications (ICRERA)*, 2016, pp. 736–741.
- [16] M. Hajizadeh and S. H. Fathi, "Selective harmonic elimination strategy for cascaded H-bridge five-level inverter with arbitrary power sharing among the cells," *IET Power Electronics*, vol. 9, no. 1, pp. 95–101, 2016.
- [17] I. Sefa, H. Komurcugil, S. Demirbas, N. Altin, and S. Ozdemir, "Three-phase three-level inverter with reduced number of switches for stand-alone PV systems," in *2017 IEEE 6th International Conference on Renewable Energy Research and Applications (ICRERA)*, 2017, pp. 1119–1124.
- [18] N. Altin, I. Sefa, H. Komurcugil, and S. Ozdemir, "Three-phase three-level T-type grid-connected inverter with reduced number of switches," in *2018 6th International Istanbul Smart Grids and Cities Congress and Fair (ICSG)*, 2018, pp. 58–62.
- [19] M. S. A. Dahidah, G. Konstantinou, and V. G. Agelidis, "A Review of Multilevel Selective Harmonic Elimination PWM: Formulations, Solving Algorithms, Implementation and Applications," *IEEE Transactions on Power Electronics*, vol. 30, no. 8, pp. 4091–4106, Aug. 2015.
- [20] A. Salem, E. M. Ahmed, M. Orabi, and M. Ahmed, "Study and Analysis of New Three-Phase Modular Multilevel Inverter," *IEEE Transactions on Industrial Electronics*, vol. 63, no. 12, pp. 7804–7813, Dec. 2016.
- [21] J. I. Leon, S. Kouro, L. G. Franquelo, J. Rodriguez, and B. Wu, "The Essential Role and the Continuous Evolution of Modulation Techniques for Voltage-Source Inverters in the Past, Present, and Future Power Electronics," *IEEE Transactions on Industrial Electronics*, vol. 63, no. 5, pp. 2688–2701, May 2016.
- [22] J. Sun and H. Grotstollen, "Solving nonlinear equations for selective harmonic eliminated PWM using predicted initial values," in *and Automation Proceedings of the 1992 International Conference on Industrial Electronics, Control, Instrumentation*, 1992, pp. 259–264 vol.1.
- [23] M. H. Etesami, N. Farokhnia, and S. H. Fathi, "Colonial Competitive Algorithm Development Toward Harmonic Minimization in Multilevel Inverters," *IEEE Transactions on Industrial Informatics*, vol. 11, no. 2, pp. 459–466, Apr. 2015.
- [24] K. P. Panda and G. Panda, "Application of swarm optimisation-based modified algorithm for selective harmonic elimination in reduced switch count multilevel inverter," *IET Power Electronics*, vol. 11, no. 8, pp. 1472–1482, 2018.
- [25] M. Etesami, D. M. Vilathgamuwa, N. Ghasemi, and D. P. Jovanovic, "Enhanced Meta-heuristic Methods for Selective Harmonic Elimination Technique," *IEEE Transactions on Industrial Informatics*, pp. 1–1, 2018.
- [26] S. S. Lee, M. Sidorov, N. R. N. Idris, and Y. E. Heng, "A Symmetrical Cascaded Compact-Module Multilevel Inverter (CCM-MLI) With Pulsewidth Modulation," *IEEE Transactions on Industrial Electronics*, vol. 65, no. 6, pp. 4631–4639, Jun. 2018.
- [27] K. P. Panda, B. P. Sahu, D. Samal, and Y. Gopal, "Switching Angle Estimation using GA Toolbox for Simulation of Cascaded Multilevel Inverter," *International Journal of Computer Applications*, vol. 73, no. 21, pp. 21–26, Jul. 2013.
- [28] M. Gnana Sundari, M. Rajaram, and S. Balaraman, "Application of improved firefly algorithm for programmed PWM in multilevel inverter with adjustable DC sources," *Applied Soft Computing*, vol. 41, pp. 169–179, Apr. 2016.
- [29] K. P. Panda, A. Anand, P. R. Bana, and G. Panda, "Novel PWM Control with Modified PSO-MPPT Algorithm for Reduced Switch MLI Based Standalone PV System," *International Journal of Emerging Electric Power Systems*, vol. 19, no. 5, 2018.
- [30] R. Guruambeth and R. Ramabadrana, "Fuzzy logic controller for partial shaded photovoltaic array fed modular multilevel converter," *IET Power Electronics*, vol. 9, no. 8, pp. 1694–1702, 2016.
- [31] N. Altin, "Single phase grid interactive PV system with MPPT capability based on type-2 fuzzy logic systems," in *2012 International Conference on*

- Renewable Energy Research and Applications (ICRERA)*, 2012, pp. 1–6.
- [32] L. M. Elobaid, A. K. Abdelsalam, and E. E. Zakzouk, “Artificial neural network-based photovoltaic maximum power point tracking techniques: a survey,” *IET Renewable Power Generation*, vol. 9, no. 8, pp. 1043–1063, 2015.
- [33] M. Killi and S. Samanta, “An Adaptive Voltage-Sensor-Based MPPT for Photovoltaic Systems With SEPIC Converter Including Steady-State and Drift Analysis,” *IEEE Transactions on Industrial Electronics*, vol. 62, no. 12, pp. 7609–7619, Dec. 2015.
- [34] G. Radhia, B. H. Mouna, S. Lassaad, and O. Barambones, “MPPT controller for a photovoltaic power system based on increment conductance approach,” in *2013 International Conference on Renewable Energy Research and Applications (ICRERA)*, 2013, pp. 73–78.
- [35] T. Atalik *et al.*, “Multi-DSP and -FPGA-Based Fully Digital Control System for Cascaded Multilevel Converters Used in FACTS Applications,” *IEEE Transactions on Industrial Informatics*, vol. 8, no. 3, pp. 511–527, Aug. 2012.
- [36] E. Babaei and S. H. Hosseini, “New cascaded multilevel inverter topology with minimum number of switches,” *Energy Conversion and Management*, vol. 50, no. 11, pp. 2761–2767, Nov. 2009.
- [37] E. Najafi and A. H. M. Yatim, “Design and Implementation of a New Multilevel Inverter Topology,” *IEEE Transactions on Industrial Electronics*, vol. 59, no. 11, pp. 4148–4154, Nov. 2012.
- [38] J. J. Nedumgatt, D. V. Kumar, A. Kirubakaran, and S. Umashankar, “A multilevel inverter with reduced number of switches,” in *2012 IEEE Students’ Conference on Electrical, Electronics and Computer Science*, 2012, pp. 1–4.
- [39] L. Wang, Q. H. Wu, and W. Tang, “Novel Cascaded Switched-Diode Multilevel Inverter for Renewable Energy Integration,” *IEEE Transactions on Energy Conversion*, vol. 32, no. 4, pp. 1574–1582, Dec. 2017.
- [40] X.-S. Yang, *Nature-inspired metaheuristic algorithms*, 2. ed. Frome: Luniver Press, 2010.
- [41] S. S. Lee, M. Sidorov, C. S. Lim, N. R. N. Idris, and Y. E. Heng, “Hybrid Cascaded Multilevel Inverter (HCMLI) With Improved Symmetrical 4-Level Submodule,” *IEEE Transactions on Power Electronics*, vol. 33, no. 2, pp. 932–935, Feb. 2018.
- [42] B. Ozpineci, L. M. Tolbert, and J. N. Chiasson, “Harmonic optimization of multilevel converters using genetic algorithms,” *IEEE Power Electronics Letters*, vol. 3, no. 3, pp. 92–95, Sep. 2005.